Journal of Engineering Science and Technology
Vol. 18, No. 5 (2023) 2587 - 2596
© School of Engineering, Taylor's University

POTENTIAL OF HYDROXYAPATITE AS A MATERIAL FOR THE SYNTHESIS OF CALCIUM TITANATE PEROVSKITE IN SOLAR CELLS

N.A. NIK AZIZ[1,*], I.Q. AFIQAH[1], S. HASIAH[2]

[1]Faculty of Fisheries and Food Science, Universiti Malaysia
Terengganu, 21030 Kuala Nerus, Terengganu, Malaysia
[2]Faculty of Ocean Engineering Technology and Informatics,
Universiti Malaysia Terengganu, 21030 Kuala Nerus, Terengganu, Malaysia
*Corresponding author: nikaziz@umt.edu.my

Abstract

In this study, Calcium titanate ($CaTiO_3$) perovskite was prepared by using two major methods which were solid-state ceramic route and mechanochemical treatment in conjunction with high-energy ball milling. The key materials to incorporate $CaTiO_3$ perovskite were marine calcium hydroxyapatite (HAp) and titanium dioxide. HAp is calcium derived from fishbone, with a chemical composition of a calcium phosphate compound. Alternatively, HAp can be a good source of natural marine calcium to replace artificial calcium. The highlight of this study is to acknowledge the ability of HAp in the production of $CaTiO_3$ which show their characteristic. $CaTiO_3$ is basically perovskite oxide with ABO_3 formula that consists of functional material which exhibits a range of stoichiometries and crystal structures. This study introduces a modification in the A-site structure to investigate the development of $CaTiO_3$ by using HAp. In addition, perovskite offers higher thermal and hydrothermal stability which enable them to be carried out at high temperatures for solid reaction and low temperatures for liquid reactions. In order to enhance our understanding of perovskite oxide synthesis, Fourier Transform Infrared Spectrometry (FTIR) and X-ray Diffraction (XRD) techniques were applied for the analysis of $CaTiO_3$. These characterizations play a pivotal role in grasping the intricacies of their structures and properties. The FTIR study shows that the functional group existed in HAp, $CaTiO_3$ and TiO_2 while XRD shows the crystallization of $CaTiO_3$. FTIR band shows the main characteristic of PO_4^{3-}, Ti-O, and $CaTiO_3$ in the ranges of 500-4000 cm^{-1}. Meanwhile, the XRD pattern shows major characteristic peaks of $CaTiO_3$ at 48.2° and 68.5° via a mechanochemical method. The findings of the study confirmed that $CaTiO_3$ formed from fishbone has a structure similar to standard $CaTiO_3$ perovskite. This research contributes to the development of methods for producing $CaTiO_3$ that can be used to bond materials which cannot be bonded using conventional methods such as biomimetic and wet precipitation.

Keywords: Calcium titanate, Hydroxyapatite, Mechanochemical treatment, Perovskite, Solid state ceramic.

1. Introduction

In recent decades, there has been significant interest among researchers in oxide thin films due to their potential to revolutionize the development of electronic devices. The advantages of oxide thin films gave exquisite optical properties that are tuneable by controlling the chemical composition and ambipolar charge transport. However, there is a higher barrier to market entry for thin-film technologies, due to higher capital costs per unit output for thin-film manufacturing facilities [1]. Hence, replacing synthetic calcium with HAp can help in reducing the material cost in the production of oxide thin films. In addition, numerous properties such as large dielectric constants, ferroelectricity, superconductivity, colossal magneto-resistance, and magneto-electric coupling effects have been discovered in oxide thin films [2]. These benefits eventually give added value to the development of oxide thin films in perovskite. Perovskite refers to oxides with the structural formula ABO_3, which evolved from $CaTiO_3$.

The coordination of the A-site and B-site cations with oxygen anions in this structure is shown in Fig. 1 [3]. The A-site cation is coordinated 12 times, whereas the B-site cation is coordinated 6 times. The structural properties of perovskite oxides indicate that the oxidation state of the B-site cation and the production of oxygen vacancies within the structure may be regulated without impacting the overall matrix structure [4]. Controlling the oxidation state of the B-site metal cation and the number of oxygen vacancies is crucial because the catalytic cycle is strongly reliant on the redox characteristics of the B-site metal cation, while oxygen vacancies offer sites for substrate adsorption and activation [5].

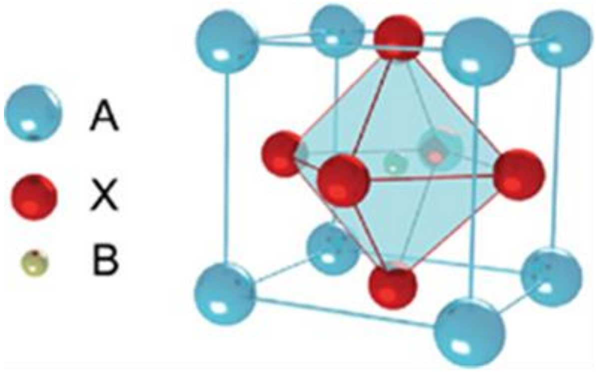

Fig. 1. Structure of perovskite.

However, to produce perovskite, the selection of materials is crucial. Many industries are impacted by the ban on materials containing toxic elements from an ecological standpoint. This restriction aims to promote environmentally-friendly practices by reducing the potential harm that such materials may cause to the environment and public health. As a result, numerous researchers are investigating the development of new non-toxic materials that possess similar or superior properties to the banned compounds. This search for alternative materials is necessary to promote sustainable and environmentally-friendly practices within various industries [6].

In order to solve this ecological problem, hydroxyapatite (HAp) had been introduced in the fabrication of $CaTiO_3$ perovskite. HAp is a calcium phosphate material with slightly bioresorbable [7] where the composition is chemically identical to the synthetic calcium. HAp can be found abundantly in fish bone waste and can be synthesized in two ways which are through inorganic components or from ordinary organic-based substances. Other than that, HAp had also been used as a catalyst in biodiesel production. The use of heterogenous catalysts is the key to eliminating the problems caused by homogenous catalysts which can be obtained mainly from fishbone waste [8]. HAp will occur at the A site cation, which has the advantage of long-term application and can be used because it is the cheapest natural calcium. It was chosen as the best material to replace synthetic calcium in the $CaTiO_3$ structure because it is the cheapest natural calcium.

Perovskite-based materials can be synthesized through a deluge of groundwork techniques. This study focuses on traditional solid-state reaction methods and mechanochemical treatment due to less chemical use and convenience. Solid state reaction method, established through soft solution chemistry methodologies such as co-precipitation, mechanochemical, hydrothermal, solverthermal, alkoxide hydrolysis, and metal–organic processing. In this study, an extraneous attempt had been put forth to find the preferred and accurate composition of $CaTiO_3$ via two fundamental methods namely solid-state ceramic route and mechanochemical processing, which generate another four methods of $CaTiO_3$ samples.

The solid-state ceramic method is commonly used for the preparation of mixed metal oxides whose textural characteristics for both starting materials are solid. The technique involves the heating of an intimate mixture of the respective binary oxides or their precursors in a solid state at high temperatures. Since both starting materials do not react at room temperature, it is necessary to supply heat until the reaction occurs at a certain temperature, mostly up to 1000 °C-1500 °C [9]. The wet medium applied for these techniques was acetone and ethanol. Ethanol is known for its ability to control the growth rates of different crystalline faces, while acetone serves as an important solvent with high properties to mix all proportions to form a homogeneous solution [10].

Mechanochemical processes, as compared to solid-state ceramic processes, use high-energy ball milling to produce ultra-fine powders in the sub-micron to the nanometre range. The reaction requires no external heat since the energy is created within the reactor by the collision of high-speed balls. This procedure is simple to use, and no harmful substances were produced. When solids are ground, crushed, or milled, the intense mechanical action can cause physical and chemical changes in the surface region of the solids. These changes can affect the properties of the material and can be either beneficial or harmful depending on the application. Understanding the effects of mechanical stress on solid surfaces is important for optimizing the properties of materials [11]. The mechanochemical effect refers to chemical and physicochemical effects in solids that are initiated by mechanical forces [12].

Researchers are studying the impact of mechanochemistry on fine particles because it has many advantages for subsequent processes. It is helping in reducing the time and temperature required for annealing and sintering, decreasing the temperature at which phase transformation occurs, improving the leaching process, lowering the temperature at which thermal decomposition occurs, and increasing the reactivity of the particles [13].

2. Materials and Methodology

The methodology employed in this study is a modified method, adapted to suit the study's requirements and based on a previous approach by [14].

2.1. Starting powders

HAp was obtained from Selayang fish bone as reported in a previous study and the process is summarized as shown in Fig. 2. Titanium dioxide was directly used without further purification in order to synthesis $CaTiO_3$.

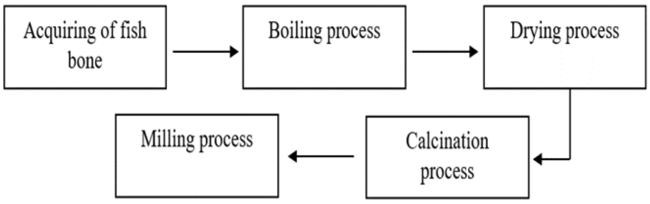

Fig. 2. Processes involved in obtaining HAp from fish bone byproduct.

2.2. Synthesis of $CaTiO_3$ through several methods

$CaTiO_3$ was synthesized using HAp as the main source of calcium and was adjusted for use according to each method, which included a solid-state ceramic route for wet medium in acetone and ethanol and a mechanochemical treatment for dry medium. The processes involved in obtaining $CaTiO_3$ are illustrated in Fig. 3.

2.2.1. Solid-state ceramic

HAp and TiO_2 were weighed in a stoichiometric ratio of 1:1 and ball mill within 6 hours at 200 rpm. For wet medium using (a) acetone and (b) ethanol, the ratio to the volume of the agate jar was 1:2. The calcination process in a medium using acetone took 8 hours and reached 1000 °C, whereas the calcination process in ethanol took only 2 hours.

2.2.2. Mechanochemical treatment

Equimolar ratios of HAp and TiO_2 in process (c) were ball milled with 1:5 ratio powders to ball in an agate jar. The milling process took 6 hours at 200 rpm. The mixed powder underwent a calcination process for 8 hours at a temperature of 1000 °C. In contrast, for procedure (d) HAp needs to be dissolved ultrasonically in deionized water for 30 minutes before adding TiO_2 to be mixed with HAp. The powder produced from procedures (a), (b), (c), and (d) was washed several times using a centrifuge to remove unreactive ions. Afterwards, the powder was dried at 80 °C for 24 hours. After removing the ion, milling for the next 2 hours was required to ensure that the starting materials were free from structural defects and mixed uniformly. The entire process was carried out using a planetary ball mill, which includes a gyratory shaft and a cylindrical jar that rotate in opposite directions at high speeds. The high rotational movement of the planetary ball mill caused the balls to move vigorously, which had a direct effect on the materials being processed [15].

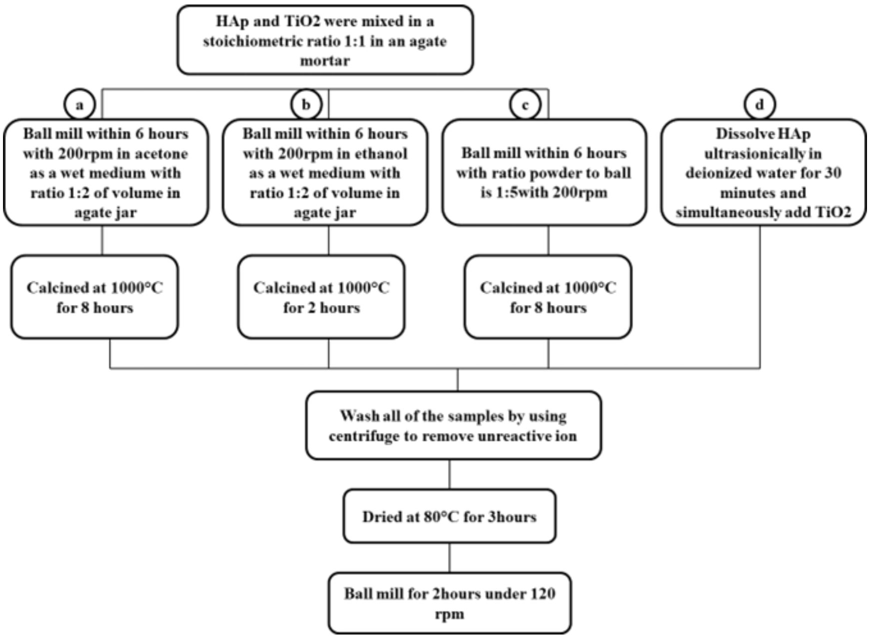

Fig. 3. Flowchart on four different methods used to synthesize $CaTiO_3$.

2.3. Characterization of $CaTiO_3$

Evaluating the samples is essential for understanding the structures and properties of the synthesized perovskite oxides. Differences in crystal or textural structure can result in variations in properties. XRD diffraction pattern was carried out by using *Cu K-α* radiations at a scanning rate of 2°/minutes to identify different phases present in the samples with different style of synthesis. For profile analysis based on relative peak intensities, the resulting patterns were adjusted to a combination of powder diffraction file (PDF) card. To support the XRD result, FTIR analysis was performed using Perkin Elmer Spectrum 400 (FTIR-ATR) between the ranges of 500-4000 cm^{-1}. In a planetary ball mill, the mixture was milled under atmospheric conditions.

3. Results and Discussion

3.1. Characterization of $CaTiO_3$

Figure 4 shows FTIR bands of the main characteristic of PO_4^{3-}, Ti-O, and $CaTiO_3$ in the ranges of 500-4000 cm^{-1} based on the various methods that had been carried out. The fundamental characteristic observed for the main characteristic is summarized in Table 1. The FTIR spectra in the range of 500-700 cm^{-1} were related to the stretching vibration of metal-oxygen. The phosphate band was observed between peaks in the range of 940-1040 cm^{-1}. The peak below 1200 cm^{-1} can be attributed to the hydroxyl group of the Ti-OH bond [16]. The weak absorption peak of the structural hydroxyl group was detected at 629.99 cm^{-1}. This indicates a strong interaction between TiO_2 and HAp [17]. As for $CaTiO_3$, the characteristic peak of the ideal cubic structure was found at 506 cm^{-1} in the process (d). The shifting of the Ti atom by the H atom, resulting in P-O-Ti type linkages, was linked to this. The stretching and bending vibrations of the BO bond in ABO_3 type perovskite materials cause the absorption bands at roughly 600 and 500 cm^{-1}. The presence of occupancy of functional groups of PO_4^{3-}, Ti-O, and $CaTiO_3$ had proven the reaction between HAp and TiO_2. In addition, HAp provided support as an electron acceptor which could promote the generation of oxygen vacancies at the interfaces with TiO_2[18].

Table 1. Functional group of major characteristic peaks of PO_4^{3-}, Ti-O, and $CaTiO_3$.

Methods		**Functional Group (cm^{-1})**		
		PO_4^{3-}	**Ti-O**	**$CaTiO_3$**
Solid state ceramic	**a) Acetone**	1026.34 972.49 945.91	1117.81	537.33
Mechanochemical treatment	**b) Ethanol**	1035.58	1093.57	517.44
	c) Dry HAp synthetic	971.58	1021.45 945.60	510.41
	d) Dry HAp	1039.08 962.29	1089.20	506.60

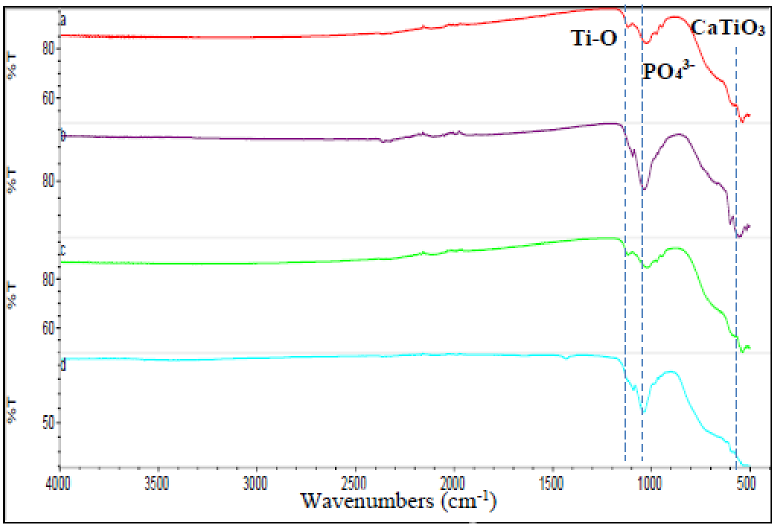

Fig. 4. FTIR spectra showing the appearance of different functional groups in different HAp-TiO_2 methods to form $CaTiO_3$.

3.2. Xray Diffraction Spectrometer Analyses (XRD)

The identification of perovskites was examined by recording the results from XRD for all samples. XRD analysis was necessary for the material investigation to identify the crystal structure. The crystallization of perovskites was then compared with the values in PDF profile data as shown in Fig. 5. In Fig. 5(a), preparation using acetone as wet medium shows high intensity of TiO_2 (rutile) peak at 27.1° (PDF 761941), overlapping of HAp (PDF 2433) and $CaTiO_3$ (PDF 82231) at 32.6° and very weak crystallization of $CaTiO_3$. In ethanol medium (Fig. 5(b)), HAp can be observed at peaks 31.7° and 49.4° (PDF 894405). When compared with acetone, the formation of $CaTiO_3$ in ethanol showed better crystallinity which was observed at 33.2°(PDF 82230). The sharp peak was contributed by TiO_2 at 27.3°.

However, in Fig. 5(c) in a dry medium, single HAp had been found at 25.7° (PDF 9432) and low crystallinity of $CaTiO_3$ was formed at 33.1°(PDF 81561). From all of the methods used, Fig. 5(d) presented major characteristic peaks of $CaTiO_3$ at 48.2° and 68.5° (PDF 22153). Pure anatase of TiO_2 was detected at 24.9° [16]. Low and rough phases of HAp indicate that the reaction between HAp and TiO_2 was at its best in this sample preparation.

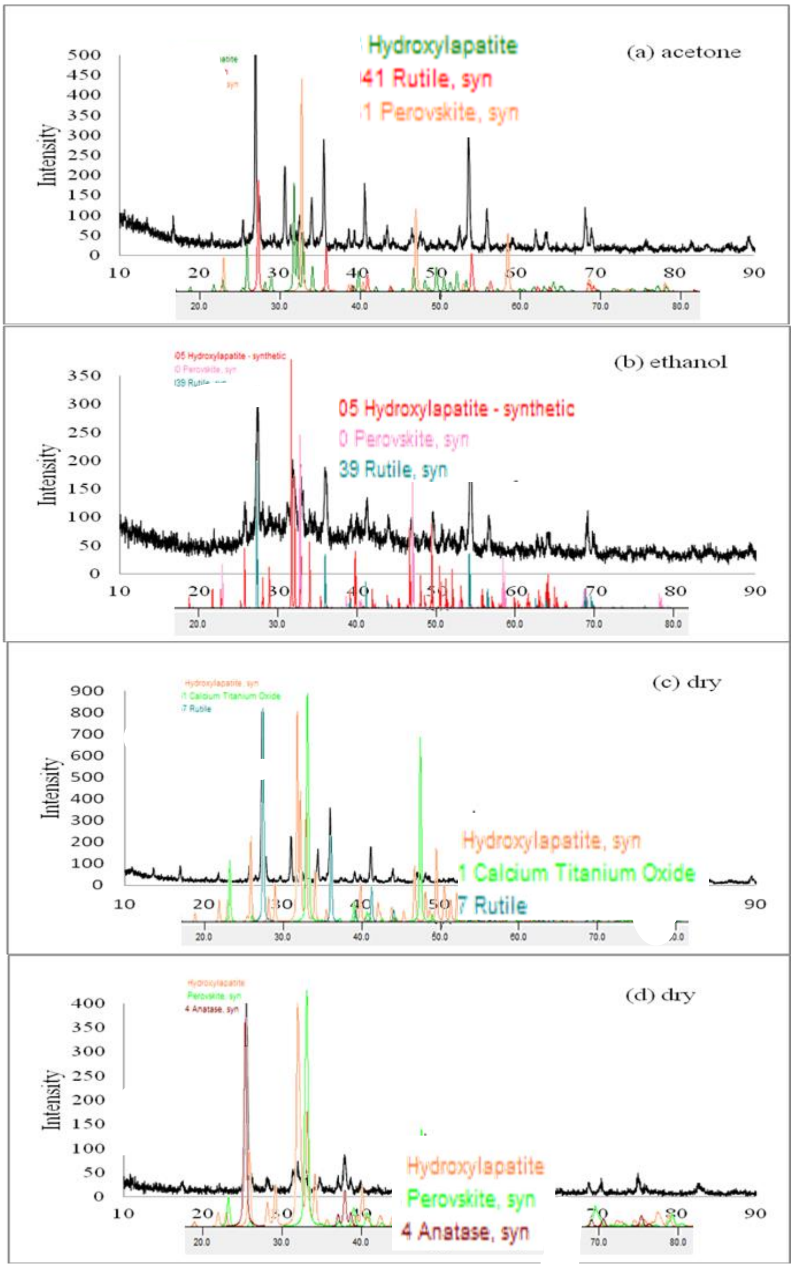

Fig. 5. XRD spectra on $CaTiO_3$ composed through several methods (a) Preparation using acetone (b) Preparation using ethanol (c) Dry preparation HAp synthetic (d) Dry preparation HAp.

4. Conclusion

This study has presented a clear methodology for producing perovskite oxides with different morphologies. It also highlighted numerous critical strategies for characterising perovskite oxides and their diverse uses. Surface areas of perovskite oxides consisting of several simple oxides are generally low. The integration of simple oxides necessitates high temperatures and lengthy calcination durations.

To improve the utilization and reactivity of perovskite oxides, it is crucial to enhance their surface area and surface properties. In theory, perovskite oxides can serve as suitable photocatalysts since the conduction and valence bands can be modified by substituting a foreign cation at either the A- or B-site. Instead of using common calcium, the A-site in this study is replaced with marine calcium HAp.

The band gap and the response to light of different wavelengths were both affected by changing this site. However, because all solid-state reaction was topotactic, using HAp as an alternative to synthetic calcium made producing $CaTiO_3$ with uniform composition more difficult. The heating condition was an essential criterion in producing quality crystalline $CaTiO_3$ powder. Interestingly, in mechanochemical synthesis, as in process (d), the FTIR and XRD results showed stability and less impurity.

After some thought and consideration, it can be concluded that the method (d-mechanochemical synthesis) produces the best $CaTiO_3$ perovskite. Mechanical energy used in the method (d) has stimulated chemical reactions and structural modification which activate minerals between the starting materials. This explains the major characteristic of $CaTiO_3$ found in this study.

Acknowledgement

The authors wish to express their gratitude to Universiti Malaysia Terengganu (UMT) for their generous support, MOHE (FRGS/1/2017/59480) for providing financial assistance under the FRGS (59480) grant, and Faculty of Fisheries and Food Science, UMT for all their technical and research support for this work to be successfully completed.

Nomenclatures

K-α	A specific type of X-ray emission

Abbreviations

$CaTiO_3$	Calcium titanate
Cu	Copper
FTIR	Fourier Transform Infrared Spectrometer
HAp	Hydroxyapatite
PO_4^{3-}	Phosphate
TiO_2	Titanium dioxide
XRD	X-ray Diffraction

References

1. Green, M.A. (2007). Thin-film solar cells: review of materials, technologies and commercial status. *Journal of Materials Science: Materials in Electronics*, 18(S1), 15-19.
2. Seo, S.S.A.; Lee, H.N.; and Noh, T.W. (2005). Infrared spectroscopy of $CaTiO_3$, $SrTiO_3$, $BaTiO_3$, Ba0. 5Sr0. $5TiO_3$ thin films, and $(BaTiO_3)$ 5/$(SrTiO_3)$ 5 superlattice grown on $SrRuO_3/SrTiO_3$ (001) substrates. *Thin Solid Films*, 486(1-2), 94-97.
3. Zhu, J.; and Thomas, A. (2009). Perovskite-type mixed oxides as catalytic material for NO removal. *Applied Catalysis B: Environmental*, 92(3-4), 225-233.
4. Zhu, J.; Li, H.; Zhong, L.; Xiao, P.; Xu, Xu.; Yang, X.; Li, J. (2014). Perovskite oxides: preparation, characterizations, and applications in heterogeneous catalysis. *Acs Catalysis*, 4(9), 2917-2940.
5. Shi, R.; Waterhouse, G.I.N.; and Zhang, T. (2017). Recent progress in photocatalytic CO_2 reduction over perovskite oxides. *Solar RRL*, 1(11), 1700126.
6. Luxová, J.; Šulcová, P.; and Trojan, M. (2008). Study of perovskite compounds. *Journal of thermal analysis and calorimetry*, 93(3), 823-827.
7. Klinkaewnarong, J.; Swatsitang, E.; Masingboon, C.; Seraphin, S.; and Maensiri, S. (2010). Synthesis and characterization of nanocrystalline HAp powders prepared by using aloe vera plant extracted solution. *Current Applied Physics*, 10(2), 521-525.
8. Rhyner, C.R.; Schwartz, L.J.; Wenger, R.B.; and Kohrell, M.G. (2017). *Waste management and resource recovery*. CRC Press.
9. West, A.R. (2014). *Solid state chemistry and its applications*. John Wiley & Sons.
10. Anthemidis, A.N.; and Ioannou, K.-I.G. (2009). Recent developments in homogeneous and dispersive liquid–liquid extraction for inorganic elements determination. A review. *Talanta*, 80(2), 413-421.
11. Darband, G.B.; Aliofkhazraei, M.; Khorsand, S.; Sokhanvar, S.; and Kaboli, A. (2020). Science and engineering of superhydrophobic surfaces: review of corrosion resistance, chemical and mechanical stability. *Arabian Journal of Chemistry*, 13(1), 1763-1802.
12. Palaniandy, S.; and Jamil, N.H. (2009). Influence of milling conditions on the mechanochemical synthesis of $CaTiO_3$ nanoparticles. *Journal of Alloys and Compounds*, 476(1-2), 894-902.
13. Palaniandy, S.; Azizli, Khairun, A.M.; Hussin, H.; and Hashim, S.F.S. (2007). Study on mechanochemical effect of silica for short grinding period. *International Journal of Mineral Processing*, 82(4), 195-202.
14. 14.Mi, Guomin.; Murakami, Y.; Shindo, D.; and Saito, F. (1999). Microstructural investigation of $CaTiO_3$ formed mechanochemically by dry grinding of a $CaO–TiO_2$ mixture. *Powder Technology*, 104(1), 75-79.
15. Pandey, A.; Jayasankar, K.; Parida, P.; Debata, M.; Mishra, BK.; and Saroja, S. (2014). Optimization of milling parameters, processing and characterization of nano-crystalline oxide dispersion strengthened ferritic steel. *Powder Technology*, 262, 162-169.

16. Comsup, N.; Panpranot, J.; and Praserthdam, P. (2010). The influence of Si-modified TiO_2 on the activity of Ag/TiO_2 in CO oxidation. *Journal of Industrial and Engineering Chemistry*, 16(5), 703-707.
17. Guo, J.; Dong, F.; Zhong, S.; Zhu, B.; Huang, W.; and Zhang, S. (2018). TiO 2–hydroxyapatite composite as a new support of highly active and sintering-resistant gold nanocatalysts for catalytic oxidation of CO and photocatalytic degradation of methylene blue. *Catalysis Letters*, 148(1), 359-373.
18. Wang, J.-D.; Liu, J.-K.; Lu, Y.; Hong, D.-J.; and Yang, X.-H. (2014). Catalytic performance of gold nanoparticles using different crystallinity HAP as carrier materials. *Materials Research Bulletin*, 55, 190-197.